

## Supplementary Information

### Combating Eukaryotic and Prokaryotic Harmful Algal Blooms with Visible-Light Driven $\text{BiOBr}_x\text{I}_{1-x}/\text{MFe}_2\text{O}_4/\text{g-C}_3\text{N}_4$ (M = Co & Ni) Photocatalysts

Anjitha A,<sup>a</sup> Shijina K,<sup>a</sup> Ajayan K. V,<sup>b</sup> Sindhu Swaminathan,<sup>a</sup> Irene M.C. Lo,<sup>c,d</sup> and Kishore Sridharan,<sup>a\*</sup>

<sup>a</sup> Department of Nanoscience and Technology, University of Calicut, P.O. Calicut University, Thenhipalam 673635, India

<sup>b</sup> Department of Botany, University of Calicut, P.O. Calicut University, Thenhipalam 673635, India

<sup>c</sup> Department of Civil and Environmental Engineering, The Hong Kong University of Science and Technology, Hong Kong, China

<sup>d</sup> Institute of Advanced Study, The Hong Kong University of Science and Technology, Hong Kong, China

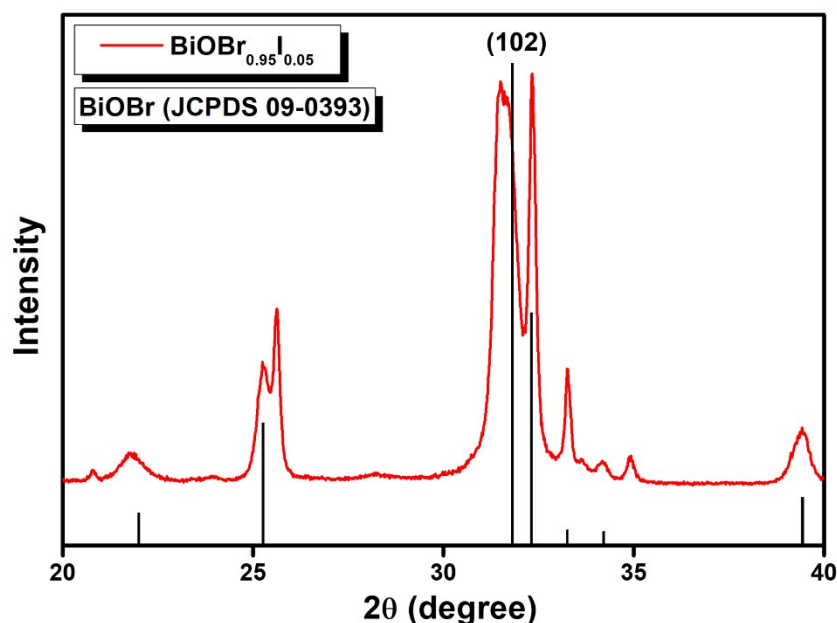


**Fig. S1** XRD pattern of  $\text{BiOBr}_{0.95}\text{I}_{0.05}$  matched with the standard JCPDS data of  $\text{BiOBr}$ . In comparison to standard  $\text{BiOBr}$ , the XRD peak of  $\text{BiOBr}_{0.95}\text{I}_{0.05}$  is observed to be shifted towards the lower angle, which could be attributed to the addition of Iodine.

---

\* Corresponding Author

Email address: [sridharankishore@uoc.ac.in](mailto:sridharankishore@uoc.ac.in) (Kishore Sridharan)

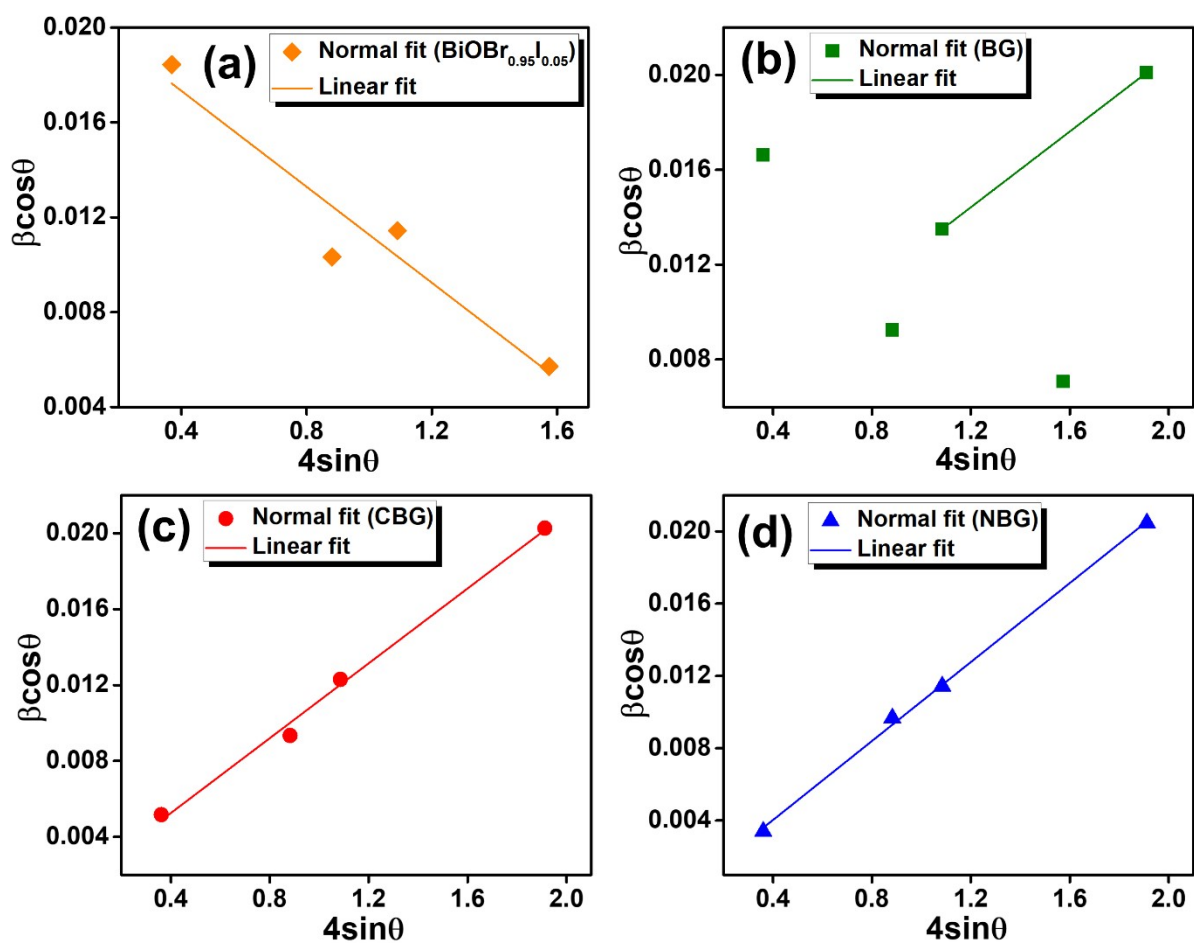


**Fig. S2.** (a-d) Plots depicting the uniform deformation model fitting (Williamson-hall method) for  $\text{BiOBr}_{0.95}\text{I}_{0.05}$  ( $\text{BBI}_{0.05}$ ), BG, CBG, and NBG, respectively.

**Table S1.** Crystallite size ( $D$ ), dislocation density ( $\rho$ ), and Internal strain ( $\epsilon$ ) calculated from the XRD data of the synthesized photocatalysts.

Photocatalyst	Crystallite size, $D(\text{nm})$	Dislocation density, $\rho = 1/D^2 (\text{nm}^{-2})$	Microstrain, $\epsilon$ (no units)
GCN	3.57	0.078	-
<b>BBI<sub>0.05</sub></b>	16.6	0.0036	-0.0101
<b>BG</b>	14.94	0.0044	0.00066
<b>CBG</b>	10.97	0.0083	0.00986
<b>NBG</b>	11.06	0.0081	0.0109

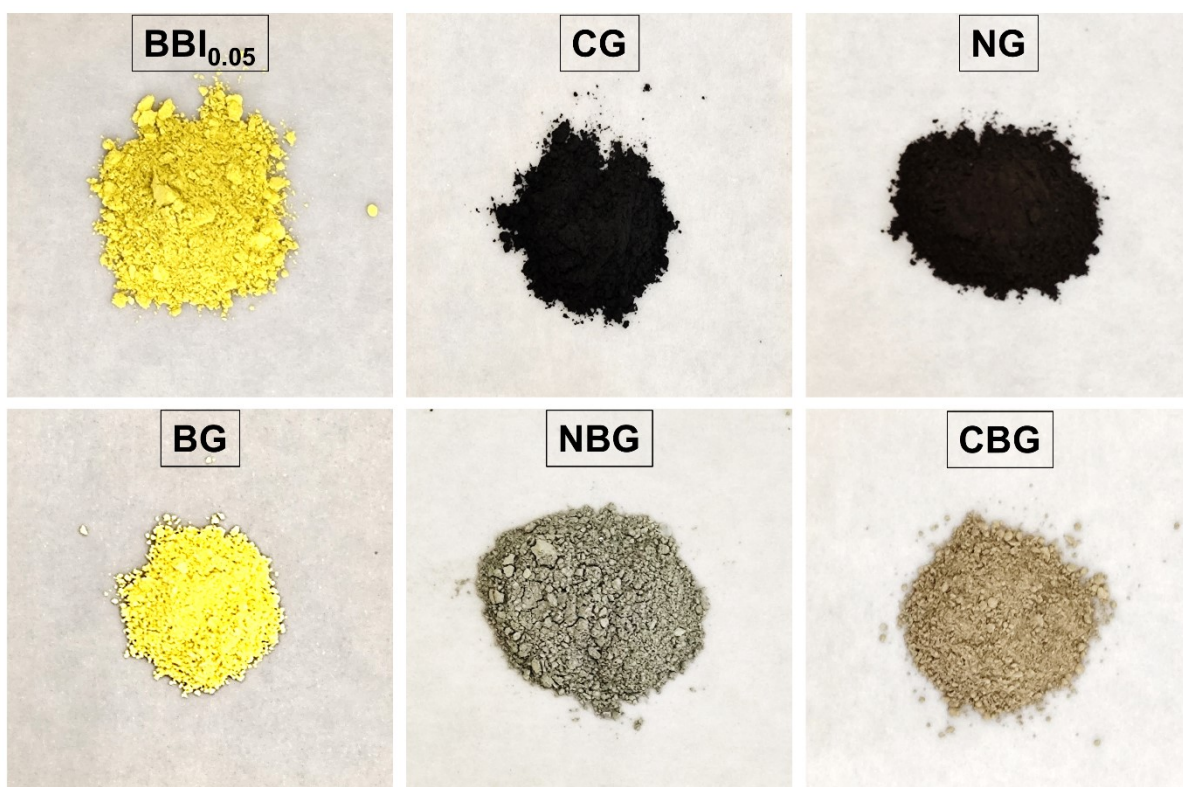


**Fig. S3.** Physical photographs of the synthesized photocatalysts.

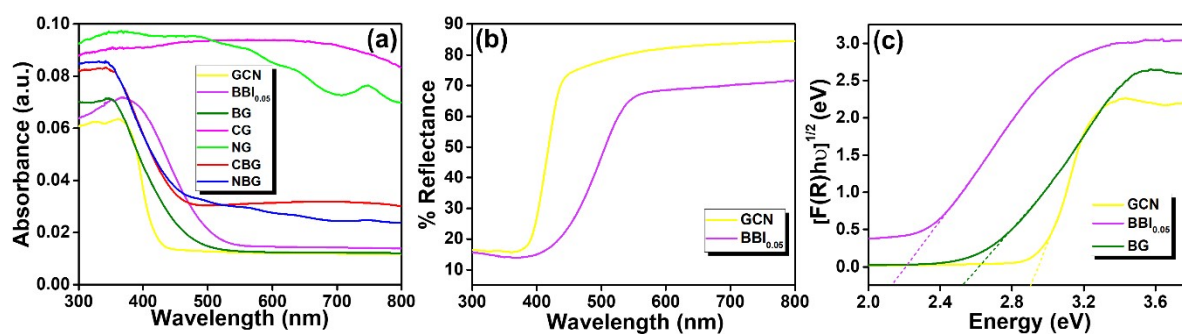


**Fig. S4.** (a) UV-vis absorbance spectra of the synthesized photocatalysts measured through DRS mode. (b) UV-vis diffuse reflectance spectra corresponding to GCN and BBI<sub>0.05</sub> photocatalysts, and (c) their corresponding Tauc plot.

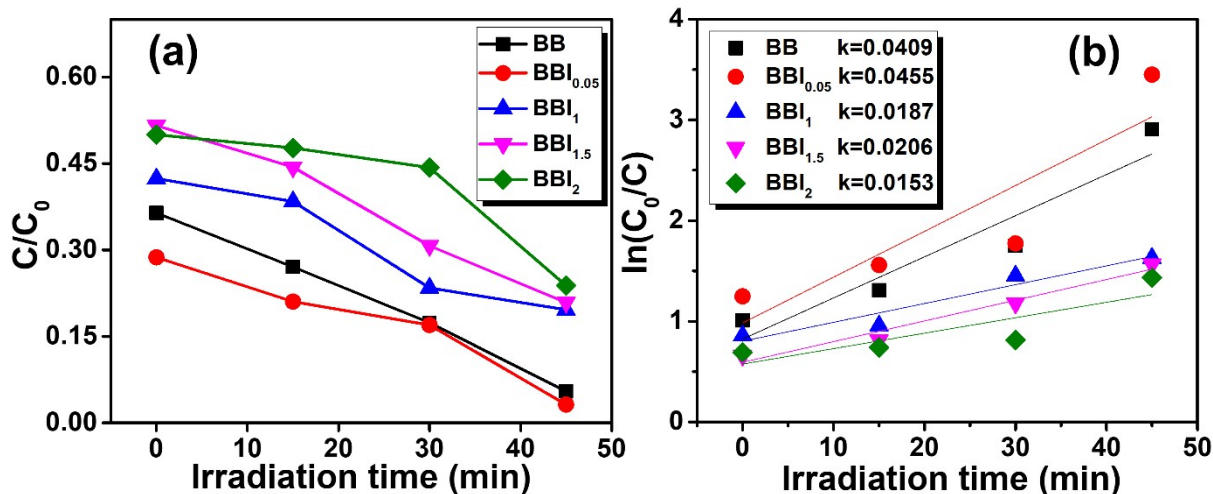


**Fig. S5.** (a) Plot depicting the time-dependent photocatalytic degradation of 5 ppm MB under visible light irradiation in the presence of BB,  $BBI_{0.05}$ ,  $BBI_1$ ,  $BBI_{1.5}$ ,  $BBI_2$ , and (b) the corresponding pseudo first-order reaction kinetic plots. The rate constants determined from the plots are mentioned in the insets.

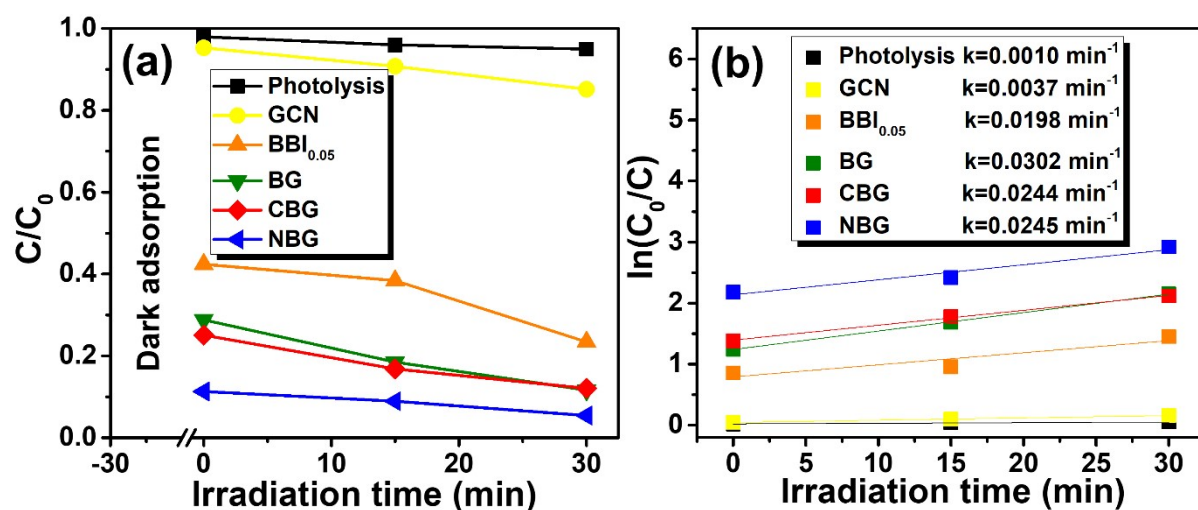


**Fig. S6.** (a) Plot depicting the time-dependent photocatalytic degradation of 5 ppm MB under visible light irradiation in the presence of  $g\text{-C}_3\text{N}_4$ ,  $BBI_{0.05}$ , BG, NBG and, CBG as photocatalysts, and (b) the corresponding pseudo first-order reaction kinetic plots. The rate constants determined from the plots are mentioned in the insets.

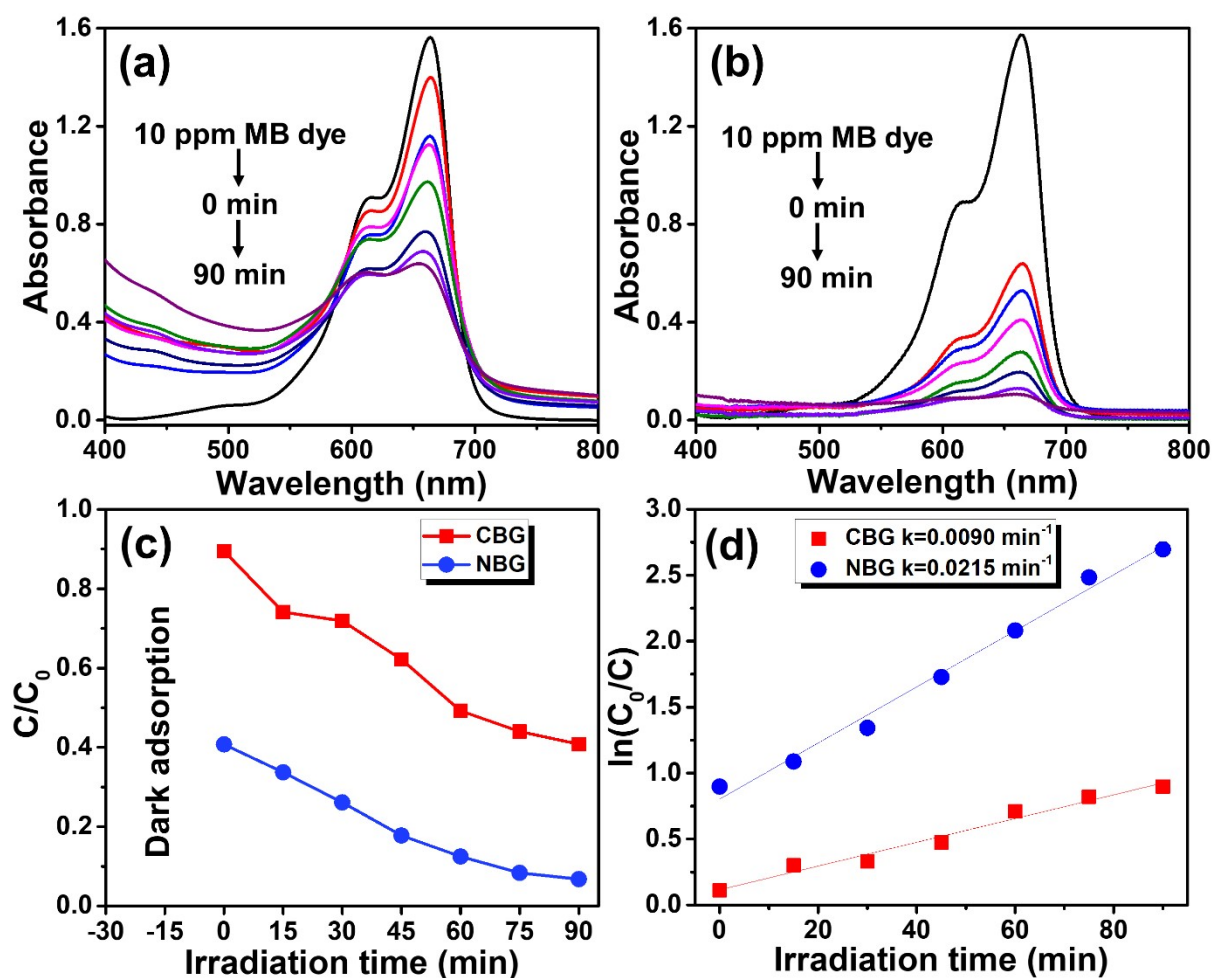


**Fig. S7.** UV-Visible absorption spectra depicting the visible light induced photodegradation of MB dye in the presence of (a) CBG and (b) NBG. (c) Plot showing the time-dependent photocatalytic degradation of 10 ppm MB under visible light irradiation in the presence of NBG and CBG, and (d) the corresponding pseudo first order kinetic plots. The rate constants determined from the plots are mentioned in the insets.

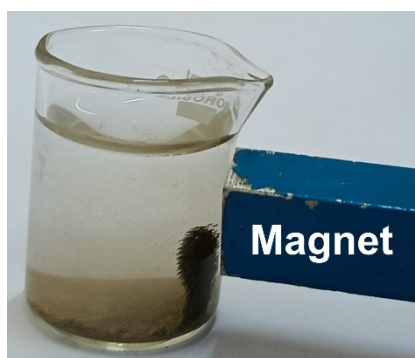


**Fig. S8.** Photograph showing magnetic separation of CBG photocatalyst from algal water.

**Table S2.** Visible light driven photodegradation of HABs in the presence of g-C<sub>3</sub>N<sub>4</sub> based heterojunction photocatalysts reported in the literature.

Photocatalyst	Details of HABs	Catalyst concentration	Light source	Degradation efficiency	Time	Ref.
<b>Bi<sub>5</sub>O<sub>7</sub>I/g-C<sub>3</sub>N<sub>4</sub></b>	<i>M. aeruginosa</i> , 4 × 10 <sup>6</sup> cells/mL	0.5g/L	500 W, Xenon lamp	99.13 %	6 h	[1]
<b>Ag<sub>2</sub>MoO<sub>4</sub>/TACN@LF</b>	<i>M. aeruginosa</i> , 4.6 × 10 <sup>6</sup> cells/mL, OD <sub>680</sub> = 0.800	6g/L	500 W, Halogen lamp	100 %	4 h	[2]
<b>Ag<sub>2</sub>O@PG</b>	<i>M. aeruginosa</i> , 4.5 × 10 <sup>6</sup> cells/mL, OD <sub>680</sub> = 0.25	0.2g/L	350 W, Xenon lamp	99.1 %	5 h	[3]
<b>Ag<sub>2</sub>O/g-C<sub>3</sub>N<sub>4</sub></b>	<i>M. aeruginosa</i> , 4.78 × 10 <sup>6</sup> cells/mL	0.5g/L	500 W, Halogen lamp	99.94 %	6 h	[4]
<b>Ag<sub>2</sub>O/g-C<sub>3</sub>N<sub>4</sub>/hydrogel</b>	<i>M. aeruginosa</i> , 4.78 × 10 <sup>6</sup> cells/mL OD <sub>680</sub> = 0.69	1 g/L	500W, Tungsten lamp	98.6 %	4 h	[5]
<b>Ag/AgCl@g-C<sub>3</sub>N<sub>4</sub>@UIO-66(NH<sub>2</sub>)</b>	<i>M. aeruginosa</i> , 3.45 mg L <sup>-1</sup> OD <sub>680</sub> = 0.82	0.3 g/L	500W, Tungsten lamp	99.9 %	3 h	[6]
<b>ZnFe<sub>2</sub>O<sub>4</sub>/Ag<sub>3</sub>PO<sub>4</sub>/g-C<sub>3</sub>N<sub>4</sub></b>	<i>M. aeruginosa</i> , 5.16 × 10 <sup>6</sup> cells/mL OD <sub>680</sub> = 0.732	1 g/L	500W, Halogen lamp	96.33 %	3 h	[7]
<b>g-C<sub>3</sub>N<sub>4</sub>/TiO<sub>2</sub></b>	<i>M. aeruginosa</i> , 2.7 × 10 <sup>6</sup> cells/mL	2 g/L	500W, Xenon lamp	88.1 %	6 h	[8]
<b>g- C<sub>3</sub>N<sub>4</sub>@Bi<sub>2</sub>MoO<sub>6</sub> @AgI</b>	<i>M. aeruginosa</i> , 4.86 × 10 <sup>6</sup> cells/mL	1 g/L	Xenon lamp	95 %	6 h	[9]

<b>Ag<sub>3</sub>PO<sub>4</sub>/g-C<sub>3</sub>N<sub>4</sub></b>	<i>M. aeruginosa</i> , 2.7 × 10 <sup>6</sup> cells/mL	0.1 g/L	Xenon lamp	90.22 %	3 h	[10]
<b>g-C<sub>3</sub>N<sub>4</sub>@EP/Al<sub>2</sub>O<sub>3</sub></b>	<i>M. aeruginosa</i> , 2.7 × 10 <sup>6</sup> cells/mL	2 g/L	500W, Xenon lamp	74.4 %	6 h	[11]
<b>g-C<sub>3</sub>N<sub>4</sub>/Bi-TiO<sub>2</sub></b>	<i>M. aeruginosa</i> , 2.7 × 10 <sup>6</sup> cells/mL	2 g/L	500W, Xenon lamp	75.9 %	6 h	[12]
<b>g-C<sub>3</sub>N<sub>4</sub>-MoO<sub>3</sub></b>	<i>M. aeruginosa</i> , 2.7 × 10 <sup>6</sup> cells/mL	1.5 g/L	300W, Xenon lamp	97 %	3 h	[13]
<b>g-C<sub>3</sub>N<sub>4</sub>@NP-TiO<sub>2</sub></b>	<i>M. aeruginosa</i> , 2.7 × 10 <sup>6</sup> cell/mL	2 g/L	500W, Xenon lamp	98.5 %	2 h	[14]
<b>BiOBr<sub>0.95</sub>I<sub>0.05</sub>/g-C<sub>3</sub>N<sub>4</sub>/CoFe<sub>2</sub>O<sub>4</sub></b>	<i>M. aeruginosa</i> , 3.85 × 10 <sup>6</sup> cell/mL OD <sub>680nm</sub> = 0.62	1 g/L	300 W, Xenon lamp	93 %	1 h	Present study
<b>BiOBr<sub>0.95</sub>I<sub>0.05</sub>/g-C<sub>3</sub>N<sub>4</sub>/CoFe<sub>2</sub>O<sub>4</sub></b>	<i>S. acuminatus</i> , 2.6 × 10 <sup>6</sup> cell/mL OD <sub>680nm</sub> = 0.77	1 g/L	300 W, Xenon lamp	98 %	1 h	Present study

## References

- [1] J. Wen, S. Sun, Q. Tang, C. Song, J. Wang, W. Zhang, L. Zhou, Y. Gao, X. Xiao, Inactivation of *Microcystis aeruginosa* under visible light by Bi<sub>5</sub>O<sub>7</sub>I/g-C<sub>3</sub>N<sub>4</sub> photocatalyst: Performance and optimization, *Chem. Eng. J.* 475 (2023) 146526. <https://doi.org/10.1016/J.CEJ.2023.146526>.
- [2] G. Fan, C. Cai, Z. Chen, J. Luo, B. Du, S. Yang, J. Wu, Visible-light-driven self-floating Ag<sub>2</sub>MoO<sub>4</sub>/TACN@LF photocatalyst inactivation of *Microcystis aeruginosa*: Performance and mechanisms, *J. Hazard. Mater.* 441 (2023) 129932. <https://doi.org/10.1016/J.JHAZMAT.2022.129932>.
- [3] Y. Chen, Z. Li, J. Wang, X. Ren, H. Feng, M. Zhang, J. Tang, X. Zhou, L. Tang, Efficient photocatalytic inactivation of *Microcystis aeruginosa* by a novel Z-scheme heterojunction tubular photocatalyst under visible light irradiation, *J. Colloid Interface Sci.* 623 (2022) 445–455. <https://doi.org/10.1016/J.JCIS.2022.04.169>.

- [4] G. Fan, B. Du, J. Zhou, W. Yu, Z. Chen, S. Yang, Stable Ag<sub>2</sub>O/g-C<sub>3</sub>N<sub>4</sub> p-n heterojunction photocatalysts for efficient inactivation of harmful algae under visible light, *Appl. Catal. B Environ.* 265 (2020) 118610. <https://doi.org/10.1016/J.APCATB.2020.118610>.
- [5] G. Fan, B. Du, J. Zhou, Z. Yan, Y. You, J. Luo, Porous self-floating 3D Ag<sub>2</sub>O/g-C<sub>3</sub>N<sub>4</sub> hydrogel and photocatalytic inactivation of *Microcystis aeruginosa* under visible light, *Chem. Eng. J.* 404 (2021) 126509. <https://doi.org/10.1016/J.CEJ.2020.126509>.
- [6] G. Fan, J. Zhan, J. Luo, J. Lin, F. Qu, B. Du, Y. You, Z. Yan, Fabrication of heterostructured Ag/AgCl@g-C<sub>3</sub>N<sub>4</sub>@UIO-66(NH<sub>2</sub>) nanocomposite for efficient photocatalytic inactivation of *Microcystis aeruginosa* under visible light, *J. Hazard. Mater.* 404 (2021) 124062. <https://doi.org/10.1016/J.JHAZMAT.2020.124062>.
- [7] G. Fan, X. Lin, Y. You, B. Du, X. Li, J. Luo, Magnetically separable ZnFe<sub>2</sub>O<sub>4</sub>/Ag<sub>3</sub>PO<sub>4</sub>/g-C<sub>3</sub>N<sub>4</sub> photocatalyst for inactivation of *Microcystis aeruginosa*: Characterization, performance and mechanism, *J. Hazard. Mater.* 421 (2022) 126703. <https://doi.org/10.1016/J.JHAZMAT.2021.126703>.
- [8] J. Song, X. Wang, J. Ma, X. Wang, J. Wang, S. Xia, J. Zhao, Removal of *Microcystis aeruginosa* and Microcystin-LR using a graphitic-C<sub>3</sub>N<sub>4</sub>/TiO<sub>2</sub> floating photocatalyst under visible light irradiation, *Chem. Eng. J.* 348 (2018) 380–388. <https://doi.org/10.1016/J.CEJ.2018.04.182>.
- [9] S. Sun, Q. Tang, T. Yu, Y. Gao, W. Zhang, L. Zhou, H. Elhegazy, K. He, Fabrication of g-C<sub>3</sub>N<sub>4</sub>@Bi<sub>2</sub>MoO<sub>6</sub>@AgI floating sponge for photocatalytic inactivation of *Microcystis aeruginosa* under visible light, *Environ. Res.* 215 (2022) 114216. <https://doi.org/10.1016/J.ENVRES.2022.114216>.
- [10] S. Sun, Q. Tang, L. Zhou, Y. Gao, W. Zhang, W. Liu, C. Jiang, J. Wan, L. Zhou, M. Xie, Exploring the photocatalytic inactivation mechanism of *Microcystis aeruginosa* under visible light using Ag<sub>3</sub>PO<sub>4</sub>/g-C<sub>3</sub>N<sub>4</sub>, *Environ. Sci. Pollut. Res.* 29 (2022) 29993–30003. <https://doi.org/10.1007/S11356-021-17857-W/FIGURES/7>.
- [11] J. Song, X. Wang, J. Ma, X. Wang, J. Wang, J. Zhao, Visible-light-driven in situ inactivation of *Microcystis aeruginosa* with the use of floating g-C<sub>3</sub>N<sub>4</sub> heterojunction photocatalyst: Performance, mechanisms and implications, *Appl. Catal. B Environ.* 226 (2018) 83–92. <https://doi.org/10.1016/J.APCATB.2017.12.034>.
- [12] J. Song, C. Li, X. Wang, S. Zhi, X. Wang, J. Sun, Visible-light-driven heterostructured g-C<sub>3</sub>N<sub>4</sub>/Bi-TiO<sub>2</sub> floating photocatalyst with enhanced charge carrier separation for photocatalytic inactivation of *Microcystis aeruginosa*, *Front. Environ. Sci. Eng.* 15 (2021) 1–12. <https://doi.org/10.1007/S11783-021-1417-3/METRICS>.
- [13] D. Wang, Y. Ao, P. Wang, Effective inactivation of *Microcystis aeruginosa* by a novel Z-scheme composite photocatalyst under visible light irradiation, *Sci. Total Environ.* 746 (2020) 141149. <https://doi.org/10.1016/J.SCITOTENV.2020.141149>.
- [14] X. Wang, X. Wang, J. Zhao, J. Song, C. Su, Z. Wang, Adsorption-photocatalysis functional expanded graphite C/C composite for in-situ photocatalytic inactivation of *Microcystis aeruginosa*, *Chem. Eng. J.* 341 (2018) 516–525. <https://doi.org/10.1016/J.CEJ.2018.02.054>.